Microstructural, Corrosion Behavior and Microhardness of Plasma Sprayed W-Ni Composite Coatings†

MORKS Magdi F.* FAHIM Narges. F.* and KOBAYASHI Akira**

Abstract

Commercial tungsten powder of average particle size 12 μm has been mixed with 10 Wt. % Ni powder and plasma sprayed on SUS304 stainless steel substrate by using a gas-tunnel type plasma spraying system. W-Ni coatings have been sprayed at different Ar plasma gas flow rates of 120, 150 and 170 l/min and different Ar carrier gas flow rates of 5, 8 and 10 l/min. The microstructure and phase structure of the sprayed coatings were investigated using scanning electron microscope (SEM), X-ray diffraction (XRD) and electron dispersive spectrometer (EDX). Corrosion tests were performed for the sprayed W–Ni coatings in 3.5 % NaCl solution using polarization measurements. It was found that the Ni-W coatings formed at higher Ar-gas flow rate are more resistant to corrosion. A more positive value of the corrosion potential and a lower value of the corrosion current are observed for coatings sprayed at higher Ar-gas flow rate.

KEYWORDS: (Plasma Spraying) (W-Ni Coatings) (Microstructure) (Hardness) (Corrosion Resistance)

1. Introduction

W-Ni composite coatings are good candidates for improving the corrosion resistance and anti-wear properties of metallic components used in the automotive industry. They are also used in magnetic storage devices and electronic industries due to the magnetic properties of Ni and W metals, as well as their high corrosion resistance. Electroplating is a well- known method used to deposit Ni coatings containing metallic [1-5] or ceramic [6-9] materials on Cu and steel substrates. Introducing W to the Ni electrodeposits increases the durability, hardness and corrosion resistance at high temperature. Although these methods have advantages such as ease of control, low cost and homogenous distribution of reinforcement particles in the metallic matrix microstructure, the coatings obtained have limited thickness (a few microns) and exhibit low adhesive strength. On the other hand, electrodepositing of these composites is limited to few metallic substrates such as Cu, Al and low carbon steel because they adhere well with these substrates. It is difficult to deposit W-Ni coatings on stainless steel substrate by electroplating methods mainly due to the poor adherence and a tendency for residual stresses to appear, which causes microcracks and hence coating failure.

Plasma spraying is a well established technique to deposit metallic or ceramic materials on metallic or nonmetallic substrates. The coatings obtained by this method are characterized by thickness ranging from a few microns to a few hundreds of microns, good adherence to substrate and superior mechanical properties. Gas-tunnel plasma spraying was developed in Osaka University [10-12] and used to deposit W-Ni coatings. This system was previously used to spray high quality ceramic and biomaterials coatings [13-16].

Microstructure, mechanical properties and corrosion resistance of plasma sprayed W-Ni composite coatings on stainless steel have not yet been studied. Many studies on the microstructure and corrosion resistance of electrodeposited Ni, Ni-W and other composites were investigated, but no studies have appeared related to plasma spraying of W-Ni coatings.

The aim of this research is to deposit W-Ni composite coatings on stainless steel substrates by using a gas-tunnel plasma spraying system. The microstructure and mechanical properties of the resulting coatings were investigated.

2. Experimental

2.1 Materials

Commercial W and Ni powders of average particle size 12 and 5 μm were used as spraying materials. Before spraying, the powders have been mixed in a ceramic pot for 30 min. The sprayed coatings were collected on SUS 304 stainless steel plates with dimensions 50x50x2.5 mm.

---

† Received on December 14, 2007
* Foreign Visiting Researcher
** Associate Professor

Transactions of JWRI is published by Joining and Welding Research Institute, Osaka University, Ibaraki, Osaka 567-0047, Japan

The substrate was grit blasted with alumina particles (100-200 μm) to roughen and clean the surface, followed by rinsing with ethanol and drying by compressed air.

2.2 Plasma spraying process

W-Ni coatings were sprayed by using a gas-tunnel type plasma spraying system. The plasma torch is composed of two copper anodes of diameter 8 mm (internal nozzle) and 20 mm (external nozzle) and one tungsten cathode. The external anode (vortex) is composed of a circular copper tube and the working plasma gas (Ar) moves inside it in a rotational flow with high velocity. A schematic diagram of gas-tunnel type plasma torch is shown in **Fig. 1**. The design of external anode (vortex) allows the plasma gases to move in a tunnel shape that affects the plasma jet shape and increase the efficiency of the spraying process. Detailed information about the structure and mechanism of this system is reported by Arata and Kobayashi [10]. The spraying parameters are listed in **Table 1**. Ar gas was used as plasma working gas as well as a carrier gas to feed the sprayed W-Ni powder inside the plasma jet. The flow rate of Ar plasma gas was varied from 120-170 l/min and carrier gas from 5 to 10 l/min to investigate the dependence of microstructure and properties of the resulting coatings on the plasma and carrier gas flow rates.

2.3 Characterization techniques

Microstructural investigation was carried out on polished cross-sections of the as-sprayed coatings. The composite coatings were cut and mounted in hot resin, followed by grinding and polishing with emery papers and finally mirror finished by buffing using an alumina slurry solution.

The morphology of coatings was observed using an ERA8800FE scanning electron microscope. Elemental analysis of the coatings was carried out using an electron dispersive spectrometer unit attached to the ERA8800FE SEM. EDX analysis was used to provide evidence of the presence of silica particles inside the coatings.

JEOL JDX-3530M X-ray diffractometer system was employed to probe the phase structure of the surfaces of as-sprayed W-Ni coatings. In the phase analysis, the radiation source was CuKα; the operating voltage was 40 kV and current 40 mA.

Hardness tests were performed on polished and buffed cross-section coated samples using an Akashi AAV-500 series hardness tester. The load used was 490.3 mN and the load time was 20 s. Each hardness value is the average of 10 readings.

2.4 Corrosion resistance measurements

Tafel polarization plots were measured by using a three-electrode corrosion cell interfaced with a potentiostat. The polarization curves were performed on an automatic polarization system of model (HSV-100 from Hokuto Denko Company, Japan). Electrochemical measurements were conducted at 25 ^{o}C. Cathodic and anodic polarization was recorded from -1.5 to + 1.5 V

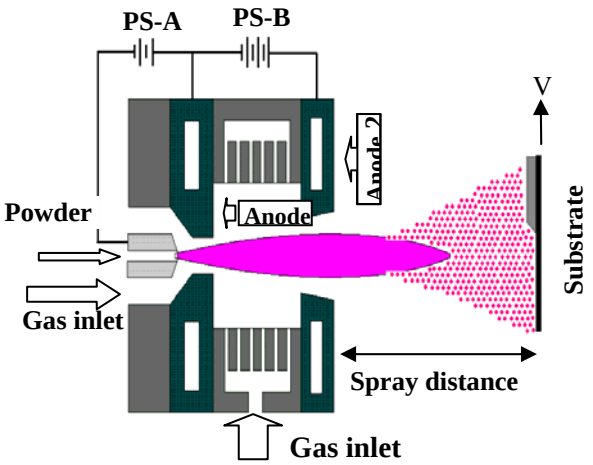

Fig. 1 Gas tunnel type plasma spraying torch.

Table 1 Spraying parameters for W-10%Ni coatings**.**

Arc gun current (A)	50
Arc vortex current (A)	300
Gas flow rate (l/min)	120, 150,170
Carrier gas flow rate (l/min)	10
Powder size (μm)	W-12, Ni-5
Spraying distance (mm)	50
Substrate traverse speed (mm/s)	40
Feeding mode	External

with sweep rate 1mV/sec in 3.5 wt % NaCl solution. The electrochemical cell consisted of Ag/AgCl as reference electrode, a platinum plate of 10 mm x 10 mm was used as counter electrode and the samples to be polarized were mounted in the substrate holder. The area of the sample exposed to the electrolyte was 0.1256 cm^2. Electrolyte solutions were prepared with analytical grade NaCl and distilled water. The polarization curve was recorded after immersion the samples for 50 min in 3.5 wt% NaCl solution.

The corrosion current density values were calculated using the Tafel slope method [17]. The Tafel's equation for the anodic over-potentials reaction ($\eta/b_a >> 1$) is defined as follows:

$$\eta = \log i_{corr} + b_a \log i \qquad (1)$$

Analogously, the Tafel's equation for the cathodic over-potentials reaction ($\eta/b_a << -1$) is defined as follows:

$$\eta = \log i_{corr} - b_c \log|i| \qquad (2)$$

The Tafel's equations predict a straight line for the variation of the logarithm of current density with potential. Therefore, currents are often shown in semilogarithmic plots known as Tafel plots. This type of analysis is referred to as Tafel slope analysis. The b_a and

b_c are the Tafel's slopes in the anodic and cathodic branches, respectively. The Tafel's slopes were estimated from the slope of the straight line portion of the Tafel's plot. However, i_{corr} and E_{corr} values were evaluated from the X and Y intercept, respectively.

3. Results & Discussion

3.1 Phase structure of W-Ni coatings

X-ray diffraction patterns of W-Ni coatings sprayed at different gas flow rates are shown in **Fig. 2**. The structure of W-Ni coatings is mainly composed of W and Ni phases as shown by the peaks corresponding to W and Ni. The crystalline peaks of W and Ni became sharp and their intensity increased as the Ar plasma gas flow rate was increased, indicating an increase in the crystallinity of W and Ni as the gas flow rate was increased. W and Ni peaks are less sharp and broadened for coatings sprayed at a gas flow rate 120 l/min, mainly due to the decrease in the plasma power level as the gas flow rate decreases. As the plasma power level decreases, the volume friction of W deposit decreases and most of the W particles are unmelted or semi-melted. As the result, a lot of pores appear and the coating becomes less dense with low crystalline phases. For W-Ni coating sprayed at 170 l/min., the peaks intensity of W phase increased compared with the Ni peaks' intensity, indicating an increase in the W amount in the coating. At high gas flow rate, the plasma power increases and leads to the increase in the flight particle temperature. That explains the increase of the volume fraction of high melting point W particles as the gas flow rate increases as shown by the increasing of W peaks intensity in Fig. 2. The above experimental results showed the influence of the plasma gas flow rate on the structure and crystallinity of the sprayed W-Ni composite coatings because of the dependence of plasma power on the plasma gas flow rate.

Figure 3 presents X-ray diffraction patterns of W-Ni coatings sprayed at different carrier gas flow rates. There are several noteworthy features in the displayed XRD patterns. The peak's intensity of W increases and that of Ni decreases as the carrier gas flow rate is increased. This may refer to an increasing in the numbers of W particles striking the substrate compared with the Ni particles because of the increase in carrier gas flow rates. The volume fraction of W was higher than that of Ni at high carrier gas flow rate.

3.2 Cross-sectional morphology and EDX analysis

Scanning electron microscope micrographs of the cross-sections of W-Ni coatings are shown in **Fig. 4**. There are bright and grey zones in the micrographs which are corresponding to W and Ni phases as detected by means of EDX elemental analysis. It was observed that, Ni particles are completely melted and diffused throughout the coatings due to the low melting point of Ni. However, unmelted W particles were recognized in the coatings sprayed at 120 l/min. due to the higher melting point of W and the low plasma power level at 120 l/min. On the other hand, the coatings became dense

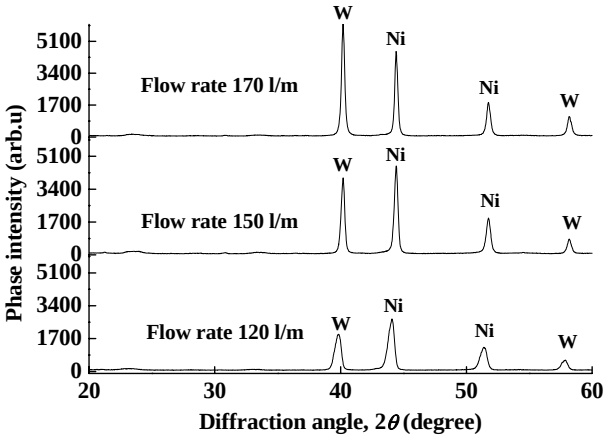

Fig. 2 X-ray diffraction patterns of W-Ni coatings sprayed at different plasma gas flow rates.

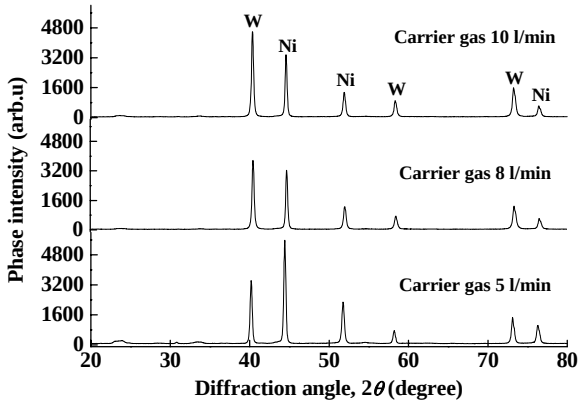

Fig. 3 X-ray diffraction patterns of W-Ni coatings sprayed at different carrier gas flow rates and plasma gas flow rate of 170 l/min.

with lower porosity as the plasma gas flow rates increased. W particles were completely or semi-melted and flattened as the flow rates increased, indicating an increase in the plasma power level and particle temperature. Generally, Ni particles were completely melted while passing the plasma jet, covered and filled between W particles and coating layers acting as a metallic binder. This description was supported by the results of EDX analysis of the cross-sectional of W-Ni coating sprayed at gas flow rate 120 l/min coatings as shown in **Fig. 5**. Although the analysis was conducted on a grey area (Ni), Ni and W spectra have been obtained, indicating the covering of the W particles by the Ni layer.

3.3 Hardness

Figure 6 presents the Vickers hardness values of W-Ni coatings sprayed at different plasma gas flow rates of 120, 150 and 170 l/min and Ar carrier gas flow rate 11 l/min. The hardness of the sprayed coatings was investigated on the cross-sectioned samples. An average of 15 points on different places of the coatings was tested. The main value of the hardness of the coatings was increased as the plasma gas flow rate was increased. The increase in hardness of the coatings with plasma gas flow

rate is referring to the decrease of the coatings porosity and increase in bonding strength of W and Ni lamella. A dense structure of the coatings sprayed at high gas flow rate (see Fig. 4 c) improves the hardness properties of the coatings.

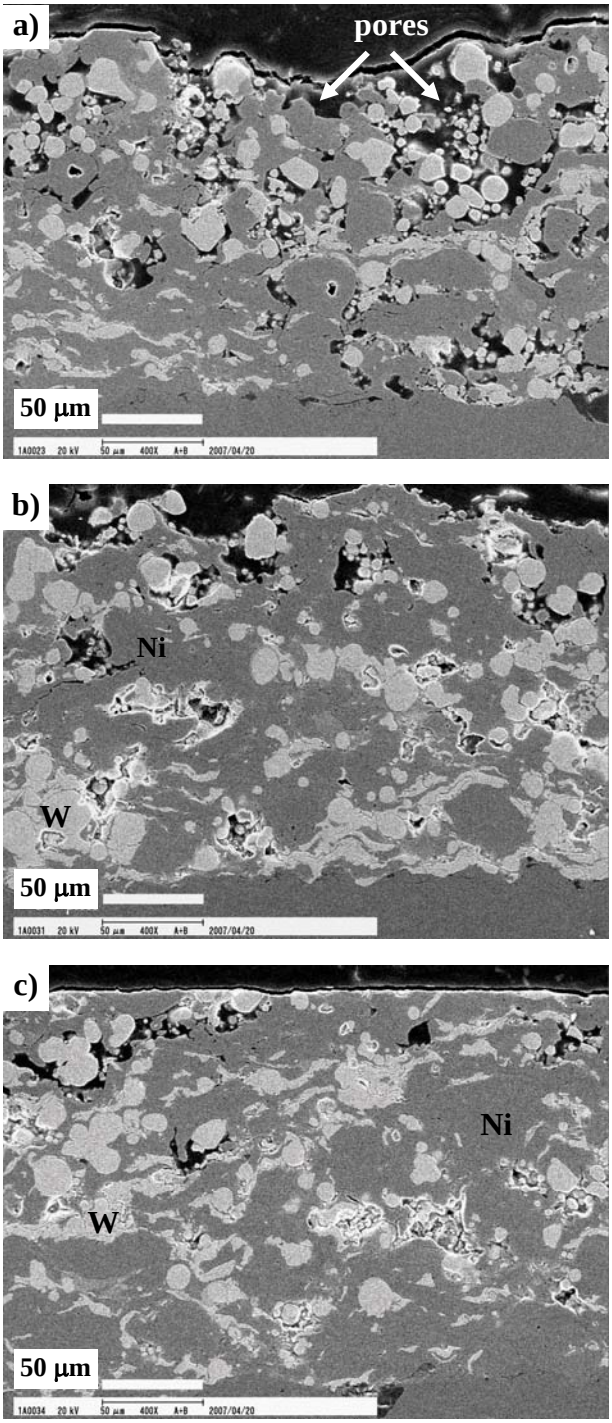

Fig. 4 SEM micrographs of polished W-Ni coatings cross-sections sprayed at different gas flow rates: a) 120 l/min., b) 150 l/min. and c) 170 l/min.

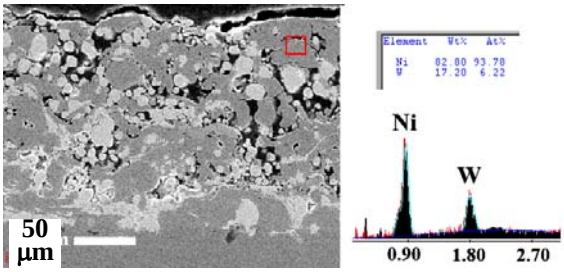

Fig. 5 EDX elemental analysis of W-Ni coating sprayed at gas flow rate 120 l/min.

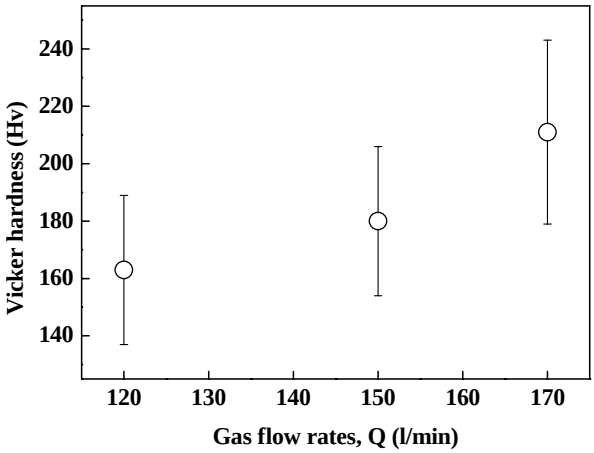

Fig. 6 Hardness values of W-Ni coatings sprayed at different gas flow rates.

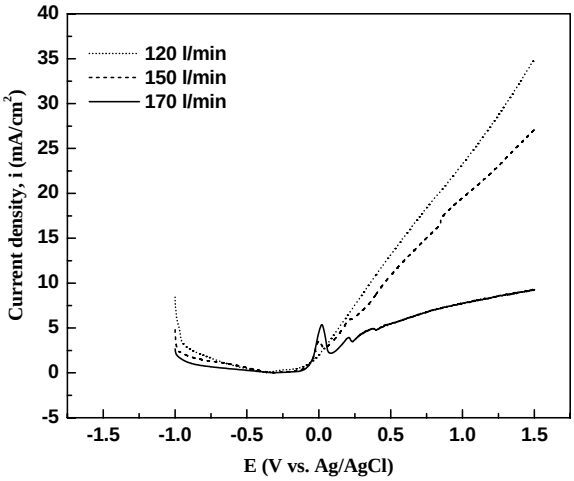

Fig. 7 Polarization curves of plasma sprayed W-Ni composite coatings at various gas flow rates in 3.5 % NaCl Solution.

3.4 Polarization behavior of W-Ni composite coatings

Figure 7 presents the polarization curves, in 3.5 % NaCl solution, of the plasma-sprayed W-Ni composite coatings deposited on SUS 304 at various Ar gas flow rates of 120, 150, and 170 l/min. The W-Ni composite coatings show an active-passive transition by polarization. It is clear that the passive current density becomes more positive as the Ar gas flow rate increases.

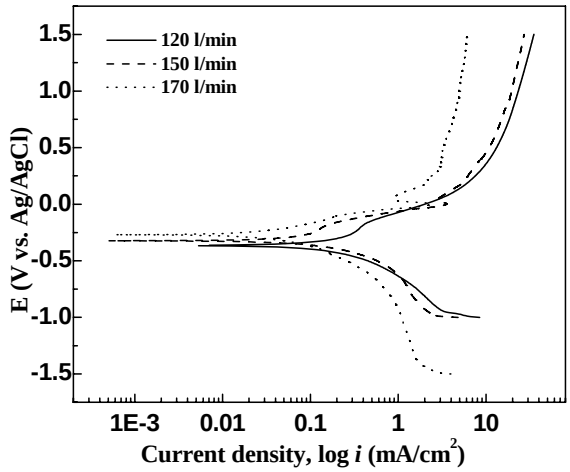

Fig. 8 Tafel's plots of plasma sprayed W-Ni composite coatings sprayed at various plasma gas flow rates in 3.5 % NaCl Solution.

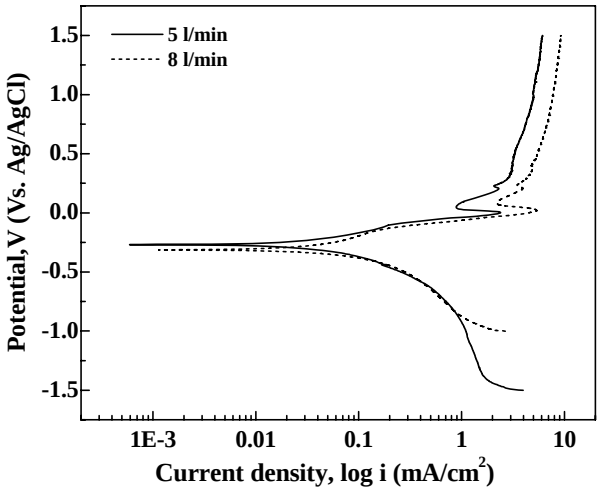

Fig. 9 Tafel's plots of plasma sprayed W-Ni composite coatings sprayed at various carrier gas flow rates of 5 and 8 l/min in 3.5 % NaCl Solution.

Table 2 Corrosion parameters of plasma-sprayed W-Ni composite coatings at various Ar gas flow rate and carrier gas.

Type of coating	E_{corr} (*V*)	i_{corr} (*mA/cm²*)
At Various Ar gas flow rate		
W-Ni coating at 120 l/min	-0.367	0.101
W-Ni coating at 150 l/min	-0.330	0.033
W-Ni coating at 170 l/min	-0.262	0.032
At Various carrier gas flow rate		
W-Ni coating at 5 l/min	-0.262	0.032
W-Ni coating at 8 l/min	-0.307	0.033

The polarization curve for the plasma-sprayed W-Ni coating at Ar flow rate 150 l/min was characterized by a small passive region extending for about 900 mV (Ag/AgCl). For the W-Ni coating sprayed at Ar gas flow rate of 170 l/min, the polarization curve shows a relatively wider passive region about 1400 mV from 100 to 1500 mV (Ag/AgCl) than that of W-Ni coating sprayed at lower Ar gas flow rate.

Tafel's extrapolation method was employed for determining corrosion current density. The resistance to corrosion of the coatings was evaluated in terms of i_{corr}. Tafel plots of the plasma-sprayed W-Ni composite coating at various Ar gas flow rate in 3.5 % NaCl solution are shown in **Fig. 8**. The i_{corr} and E_{corr} values for coatings are listed in **Table 2**. The corrosion resistance of W-Ni composite coatings was improved as the Ar gas flow rate increased. This is ascribed to the increasing the W content in the coatings as the Ar flow rate increased. The improvement in the corrosion resistance of the composite coatings may be attributed to the favorable chemical stability of W, which acts as barriers for the corrosion process by reducing the holes and gaps on the surface of composite coating and consequently preventing the corrosive pits from growing up. It is seen that the corrosion current is lower and the value of the corrosion potential is more positive for the composite coating sprayed at gas flow rate of 170 l/min, as shown in Table 2. Clearly, the W-Ni coatings sprayed at Ar gas flow rate 170 l/min have lower positive potential and smaller corrosion current densities, indicating that these coatings have lower chemical activity and hence better chemical stability in the external environment. Hui et al. [18] have mentioned the effect of tungsten in enhancing the corrosion resistance of brush plated 65Ni–28Fe–6W–1P deposit compared to electrodeposited nickel.

Figure 9 shows the Tafel's plots for W-Ni composite coatings formed at different carrier gas flow rates of 5 and 8 l/min at the same Ar gas flow rate. Clearly, the W-Ni coating sprayed at a carrier gas flow rate 5 l/min has better corrosion resistance (lower corrosion current and more positive potential) than a coating formed at higher carrier gas flow rate, as shown in Table 2. This could be attributed to the fast carrier gas makeing the tungsten particles pass rapidly and consequently, became not completely melted and causing a pores in the coating. Hence, these pores enhance the pitting corrosion.

4. Conclusions

W-Ni coatings were plasma sprayed on SUS 304 substrate using a gas-tunnel plasma spraying system. Morphology, phase structure, hardness and corrosion resistance have been investigated. The experimental results are summarized as follows:

(1) Phase structure by XRD showed that the coatings are composed of Ni and W phases and the crystallinity of both phases increased as the gas flow rate was increased.

(2) Cross-sectional morphology by SEM showed unmelted W particles inside the coating sprayed at

120 l/m because the plasma power level decreased. The coatings became dense and W amount increased as the plasma gas flow rate increased.

(3) The hardness value of the coatings increases with an increasing of plasma and carrier gas flow rates because the coatings became dense with low porosity.

(4) The corrosion resistance of the plasma-sprayed W-Ni coatings was investigated by polarization method. A more positive value of the corrosion potential and a lower value of the corrosion current were observed for coatings sprayed at higher Ar-gas flow rate.

(5) The improvement of the corrosion resistance was attributed to the W particles, which have favorable chemical stability and hence reduce the active surface area of the coatings.

Acknowledgments

The authors express their thanks to Smart Processing Research Centre in Osaka University for the provision of a gas tunnel type plasma system and characterization techniques.

References

1) T. Yamasaki, P. Schloßmacher, K. Ehrlich, Y. Ogino, Formation of amorphous electrodeposited Ni–W alloys and their nanocrystallization, Nanostruct. Mater. 10 (1998) 375–388.
2) K.R. Sriraman, S.G.S. Raman, S.K. Seshadri, Synthesis and evaluation of hardness and sliding wear resistance of electrodeposited nanocrystalline Ni–W alloys, Mater. Sci. Eng. A 418 (2006) 303–311.
3) A. Serek, A. Budniok, Electrodeposition and thermal treatment of nickel layers containing titanium, J.Alloys Compd 352 (2003) 290−295.
4) M. Popczyk, A. Budniok, A. Lasia. Electrochemical properties of Ni−P electrode materials modified with nickel oxide and metallic cobalt powders. Int. J. Hydrogen Energy 30 (2005) 265−271.
5) M. Popczyk, A. Budniok, E. Łągiewka, Structure and corrosion resistance of nickel coatings containing tungsten and silicon powders, Materials Characterization 58 (2007) 371−375.
6) M.F. Morks, N.F. Fahim, A. A. Francis, M. A. Shoeib, Fabrication and Characterization of Electo-Codeposited Ni/Zr-silicate Composite Coating, Surface and Coating Technology, 201, Issues 1-2 (2006) 282-286.
7) L.M. Chang, M.Z. An, S.Y. Shi, Microstructure and characterization of Ni-Co/Al_2O_3 composite coatings by pulse reversal electrodeposit, Materials Chemistry and Physics 100 (2006) 395–399.
8) Min-Chieh Chou, Ming-Der Ger, Shih-Tsung Ke, Ya-Ru Huang, Shinn-Tyan Wu, The Ni–P–SiC composite produced by electro-codeposition, Materials Chemistry and Physics 92 (2005) 146–151.
9) K. H. Hou, M. D. Ger, L. M. Wang, S. T. Ke, The wear behaviour of electro-codeposited Ni–SiC composites, Wear 253 (2002) 994-1003.
10) Y. Arata, A. Kobayashi, Application of gas tunnel to high energy density plasma beams. J. Appl. Phys. 59 (9) (1986) 3038–3044.
11) A. Kobayashi, New applied technology of plasma heat sources, Weld. International 4 (4) (1990) 276–282.
12) A. Kobayashi, T. Kitamura, Effect of heat treatment on high-hardness zirconia coatings formed by gas tunnel type plasma spraying, Vacuum 59 (2000) 194-202.
13) N.F. Fahim and A. Kobayashi, Gas tunnel type plasma spraying deposition and microstructure characterization of silicon carbide films for thermoelectric applications, Materials Letters 60 (2006) 3838-3841.
14) M.F. Morks, A. Kobayashi, Influence of gas flow rate on the microstructure and mechanical properties of hydroxyapatite coatings fabricated by gas tunnel type plasma spraying, Surf. Coat. Technol. 201 (2006) 2560–2566.
15) M.F. Morks, A. Kobayashi, N.F. Fahim, Abrasive wear behavior of sprayed hydroxyapatite coatings by gas tunnel type plasma spraying, Wear 262 (2007) 204–209.
16) M.F. Morks, A. Kobayashi, Gas tunnel plasma spraying of bio-gradient HA/ZrO_2 Coatings, In: Proceeding of the 14th annual meeting of Institute of Applied Plasma Science IAPS (2007) Sendai-Japan.
17) C.M.A. Brett, A.M. Oliviera Brett, Electrochemistry: Principles, Methods and Applications, Oxford University Press, 1998.
18) W.H. Hui, J.J. Liu and Y.S. Chaug, Surf. Coat. Technol. 68/69 (1994) 546–551.